

PAPER • OPEN ACCESS

The beam stop as an intensity monitor

To cite this article: L Müller *et al* 2022 *J. Phys.: Conf. Ser.* **2380** 012081

View the [article online](#) for updates and enhancements.

You may also like

- [Operating synchrotron light sources with a high gain free electron laser](#)
S Di Mitri and M Cornacchia
- [AMO science at the FLASH and European XFEL free-electron laser facilities](#)
J Feldhaus, M Krikunova, M Meyer et al.
- [Compact XFEL and AMO sciences: SACLA and SCSS](#)
M Yabashi, H Tanaka, T Tanaka et al.

ECS Toyota Young Investigator Fellowship



For young professionals and scholars pursuing research in batteries, fuel cells and hydrogen, and future sustainable technologies.

At least one \$50,000 fellowship is available annually.
More than \$1.4 million awarded since 2015!



Application deadline: January 31, 2023

Learn more. Apply today!

The beam stop as an intensity monitor

L Müller¹, M Walther¹, M Riepp¹, A Philippi-Kobs¹, W Jo¹,
W Roseker¹, K Bagschik^{1,2}, R Frömter², R Pan¹, D Lott³, J Möller⁴,
U Bösenberg⁴, J Hallmann⁴, A Rodriguez-Fernandez⁴, M Scholz⁴,
G Ansaldi⁴, J Wrigley⁴, A Zozulya⁴, A Madsen⁴ and G Grübel¹

¹ Deutsches Elektronen-Synchrotron DESY, Notkestraße 85, 22607 Hamburg Germany

² Institut für Nanostruktur- und Festkörperphysik, University Hamburg,
Luruper Chaussee 149, 22761 Hamburg, Germany

³ Forschungszentrum Hereon, Max-Planck-Straße 1, 21502 Geesthacht, Germany

⁴ European XFEL, Holzkoppel 4, 22869 Schenefeld, Germany

E-mail: leonard.mueller@desy.de

Abstract. Free-electron lasers (FELs) provide unique possibilities in investigating matter down to femtosecond time and nanometer length scales, as well as in the regime of non-linear light–matter interaction. Due to the nature of FEL sources, the produced beam is significantly more unstable than beams produced by 3rd generation synchrotrons. As a result, pulse-resolved normalization of measurement data becomes essential and can be challenging. The intensity monitors permanently installed at a facility might indeed accurately measure the pulse intensities at a certain point of the beamline, but cannot precisely normalize experimental data. For example the impact of pointing instabilities and hence different clipping of the beam downstream on the way to the actual experiment is not reflected in the intensity measurement. Here, we show how the integral intensity of the FEL beam transmitted through the sample can be measured by photodiodes providing a proper normalization of measurement data.

1. Introduction

Free-electron lasers (FELs) have brought about exciting new possibilities in investigating structural and electronic properties, particularly dynamics, in a wide variety of systems [1]. With their gain in peak photon flux as compared to state-of-the-art storage-ring sources they also allow for entirely new experiments including the study of X-ray induced non-linear effects [2–4]. Yet, the increase in peak power comes at the price of losing the stability that is readily available nowadays at synchrotron sources. While at synchrotrons the beam position and intensity may easily be stable over hours, at an FEL, the pulse intensity inherently fluctuates and might be accompanied by a considerable pointing jitter. This may, by clipping at pinholes, add to the pulse-to-pulse power fluctuation at the sample position. For experiments looking purely at structure, like in bioimaging, pulse-intensity fluctuations might be of secondary importance, as a large data set containing tens of thousands of images has to be filtered considering a number of criteria, of which pulse intensity is just one. Other techniques, however, rely on measuring consecutive frames and conclusions are drawn from relative changes between single exposures. For such techniques a reliable normalization of the data is essential.

While usually at FEL sources devices exist that can measure the intensity pulse by pulse, in some cases, their data is not usable in certain experiments. For example, FLASH at DESY



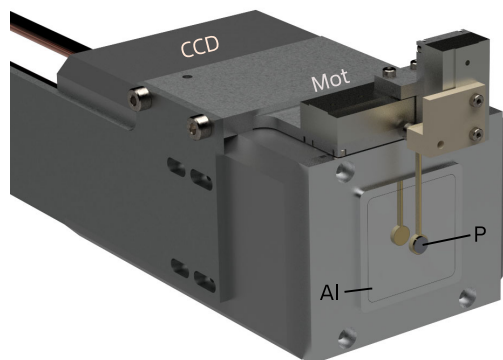


Figure 1. Beam-stop assembly used at BL3 at FLASH. A bare XUV-sensitive photodiode (P) (an SXUV5 chip obtained as custom product from OptoDiode) was bonded to a vacuum-compatible circuit board. This beam-stop photo-diode was attached via an insulating adapter piece to a two-axis piezo stage (Mot) that allows accurate positioning millimeters away from a 100 nm thin aluminum filter (Al) shielding the CCD chip from any residual light.

uses gas monitor detectors (GMD) to determine the pulse intensity way upstream of the experiment [5]. However, due to the upstream location, the GMD cannot account for intensity losses that occur during beam transport due to pointing instabilities leading to clipping at apertures. Even larger fluctuations of the pulse intensity at the sample position that cannot be measured by upstream intensity monitors are produced if a monochromator is used after the intensity monitor. Due to the fluctuating central photon energy that naturally occurs especially in all SASE FEL sources [6], the monochromator transmission varies from pulse to pulse which leads to only a weak correlation of pulse intensities before and after a monochromator.

Here, we show two solutions how the beam stop, that protects an area detector from the direct FEL beam in a small-angle scattering (SAXS) experiment, can be used to reliably extract the intensity of the beam transmitted through the sample, therewith providing a proper means of normalizing the data. First, for experiments in the extreme ultraviolet (XUV) regime at beam line BL3 [5] at FLASH at DESY, Hamburg, we used a fast XUV-sensitive photodiode as beam stop mounted directly in front of the CCD detector. Second, in the hard X-ray regime, in an experiment at the MID instrument [7] at European XFEL, Schenefeld, we used a photodiode detecting stray radiation from a slanted tantalum beam stop mounted on the exit window of the beamline, centimeters in front of the detector. We note here that measuring the intensity of the transmitted beam might be problematic in certain cases. For example, if the sample scatters strongly, such that a significant portion of the beam might or might not be scattered depending on other non-constant experimental parameters, or if the incoming FEL intensity is so high that the absorption of the sample is altered by non-linear effects [8, 9]. These restrictions do not apply for the experiments in which we tested our intensity monitors.

2. Experimental

The first implementation of the beam-stop intensity monitor was realized for an experiment at FLASH beam line BL3 [5], where we installed a custom-made end station. The FEL photon energy was tuned to ≈ 60 eV, resonant to the Co $M_{2,3}$ edge in order to measure resonant magnetic small-angle scattering (mSAXS). For the experiment, we used the unmonochromatized beam that was strongly attenuated so that the pulse energy at the sample did not exceed $1 \mu\text{J}$ such that the sample was not altered by the FEL beam. Due to the small penetration depth of photons at $E_{\text{ph}} = 60$ eV we used a fast XUV sensitive photodiode as beam stop. The bare chip with an active area of 5 mm in diameter was bonded to a vacuum-compatible circuit board to extract the signal. This assembly was used as beam stop (Fig. 1). The beam-stop assembly (photodiode and circuit board) was mounted on a two-axis piezo stage attached directly to the CCD detector, allowing accurate positioning of the beam stop in the detector plane. Only millimeters downstream of the beamstop an aluminum filter was mounted to protect the CCD sensor from any residual visible light and, importantly, from the infra-red (IR) stray radiation of the pump laser used to excite the sample. For the beam-stop photodiode no shielding was

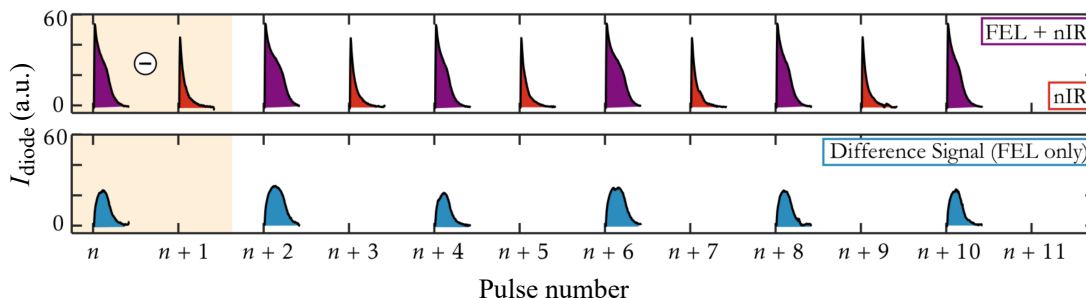


Figure 2. Pulse structure measured by the beam-stop photodiode. *top panel:* The IR laser pumps the sample at a repetition rate of 10 Hz, while the FEL repetition rate is 5 Hz. *bottom panel:* Subtracting the consecutive IR-laser signal (at $n + 1, n + 3, \dots$) from the combined IR-laser and FEL signal (at $n, n + 2, \dots$) provides a measure for the relative intensity fluctuations of the FEL at the sample position that can be used for normalization of the scattering data.

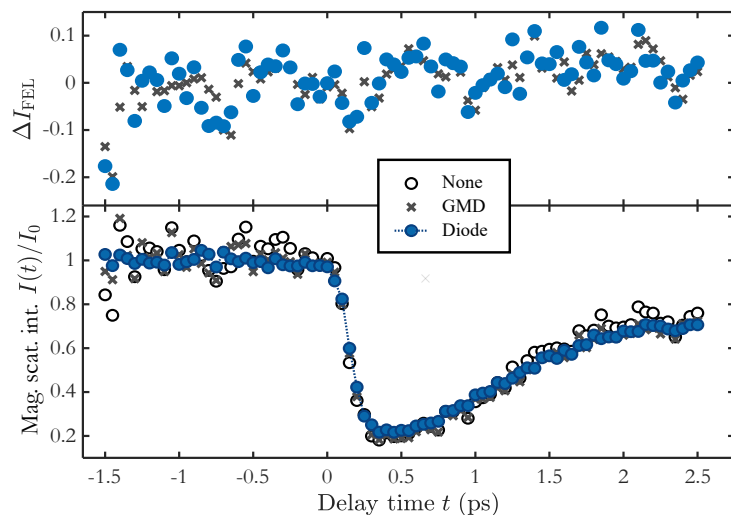


Figure 3. *top panel:* FEL intensity variation $\Delta I_{\text{FEL}} = I/\bar{I} - 1$ measured by the GMD and beam-stop photodiode both averaged over 100 pulses (\bar{I} = mean intensity). *bottom panel:* Magnetic scattering intensity $I(t)/I_0$ as a function of pump-probe delay time (I_0 = mean intensity at negative delays). The FEL intensity variations lead to noise in the unnormalized data ('none'). Normalization to the photodiode signal is superior to normalization to the GMD signal.

possible as any filter holder would have increased the effective size of the beam stop, cutting the scattering signal on the detector in the low- q region around the beam stop. Hence, the beam-stop photodiode records a summed signal containing the contributions of the IR pump laser and the FEL signal. From this combined signal the FEL signal has to be extracted. From a measurement of the signal generated by the IR laser alone it turns out that its intensity is very stable ($\pm 1\%$ around the mean), such that it was possible to subtract it from the combined signal. In the experiment, we reduced the FEL repetition rate to 5 Hz using the FLASH fast shutter [5] while the IR laser repetition rate was 10 Hz. Hence, the signal, recorded by the FLASH 100 MHz analogue-to-digital converter (ADC), contains alternating combined and IR-only transients (Fig. 2, upper panel). Subtracting subsequent transients as indicated yields the FEL intensity that can be used for normalization (Fig. 2, lower panel).

To demonstrate the performance of the beam-stop photodiode as a normalization device, we show data from an mSAXS experiment studying ultrafast demagnetization [10] in Co/Pt multilayer systems, a research topic that has greatly benefited from the advent of FELs [11]. In short, nanoscopic magnetic domains in a Co/Pt multilayer system give rise to mSAXS and the resulting scattering pattern contains information on the magnetization of the sample. This is related to the square root of the scattering intensity I , as well as on the distribution of length scales encoded in the scattering pattern's form and position in q space. Scientific results of the

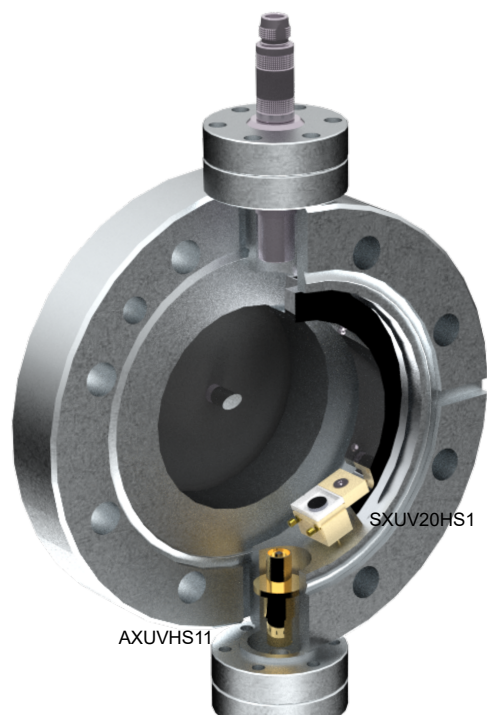


Figure 4. Beam stop and photodiode assembly used at the MID instrument at European XFEL. The beam stop is cut from tantalum with a 30° slanted surface to increase the footprint of the beam on its surface and at the same time increase the signal in the two photodiodes (AXUVHS11 and SXUV20HS1 from OptoDiode) taking also into account the polarization of the X-rays which is horizontal. The tantalum beam stop is welded to a disc made of a highly magnetic 49% cobalt-iron alloy that, in turn, is glued to the exit window made from $80\ \mu\text{m}$ thick black Kapton that in turn is glued to a custom made CF63 flange using two-component epoxy glue. The beam stop's magnetic base allows a permanent magnet to be attached from the air side as counterbalance so that the beam stop is straight.

measurement campaign will be published elsewhere [12].

The measurements were done in a multi-shot mode, collecting the scattering signal from 100 FEL pulses in one exposure of the CCD detector and, consequently, the corresponding 100 FEL transients measured from the beam-stop photodiode were averaged to generate the normalization signal (Fig. 3). The top panel shows the FEL intensity as measured upstream in the end of the undulator tunnel by the GMD as well as measured by the beam-stop photodiode. The photodiode indicates larger variations than the GMD signal. Note that even after summing up the intensity transients of 100 individual FEL pulses, as it is done here, a considerable fluctuation in the average pulse intensity remains.

Indeed, normalizing the scattering data to the signal from the beam stop photodiode is superior to normalization to the GMD signal (Fig. 3 lower panel). Residual intensity variations are a factor 2 smaller in case of normalization to the photodiode. We note that raw data points with particularly high or low intensity still are outliers when normalizing to the GMD data, which is clearly reduced when normalizing to the beam-stop photodiode signal.

In a different approach, designed for hard X-ray energies in the range of 8 keV for use at the MID instrument [7] of the European XFEL, we use photodiodes to detect stray radiation from a slanted tantalum beam stop glued onto a black Kapton window, shielding the photodiodes from visible light entering the vacuum chamber from the outside (Fig. 4). A detector (ePix) was placed in air behind the Kapton window to detect scattering at very low q . However, for this demonstration, data from the AGIPD detector installed upstream of the beamstop is used. We used a AXUVHS11 and a SXUV20HS1 photodiode from OptoDiode mounted on an SMA feedthrough or a PEEK holder, respectively, inside the CF63 flange assembly $\approx 40\ \text{mm}$ away from the beam stop. The FEL was set to deliver single pulses at a repetition rate of 10 Hz at a photon energy of 7.79 keV and the beam was monochromatized by the MID monochromator using Si(111) crystals. As only photons scattered by the beam stop are detected, the signal from the AXUV diode with an active area of only $0.28\ \text{mm}^2$ was too noisy to be reliable for

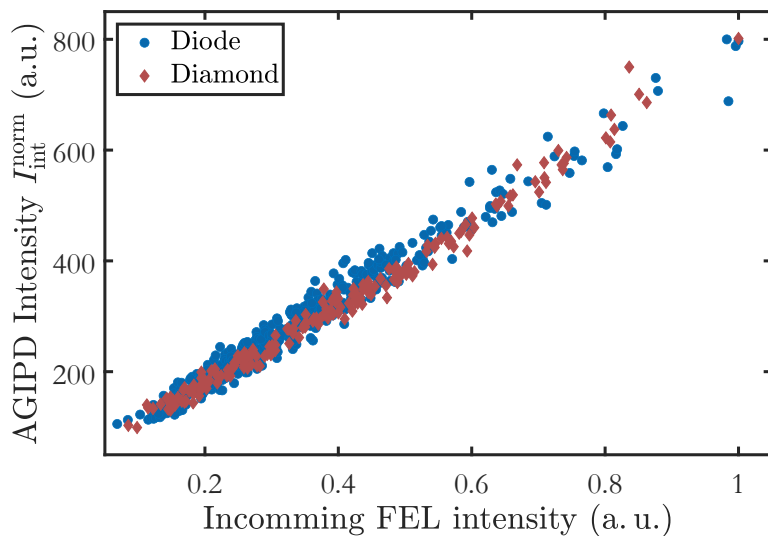


Figure 5. Total scattering intensity $I_{\text{int}}^{\text{norm}}$ of a calibration sample, $\text{Li}_4\text{Ti}_5\text{O}_{12}$ enclosed in Kapton, measured on the AGIPD detector plotted versus the normalization signal from a diamond detector upstream of the sample and from the large beam-stop photodiode, respectively.

normalization. Instead, the signal from the SXUVH20HS1 diode with an active area of 25 mm^2 was amplified and fed into a slow ADC of the MID beamline. In order to check the performance of the assembly we used a diamond detector [13] upstream of the sample position as another source of normalization. To demonstrate the validity of these normalization signals, we used a calibration sample, $\text{Li}_4\text{Ti}_5\text{O}_{12}$ enclosed in Kapton. This sample produced a pronounced, broad small-angle scattering ring around $q = 0.4\text{ \AA}^{-1}$ and a Debye-Scherrer ring at $q \approx 1.3\text{ \AA}^{-1}$, close to the maximum q observable in the used configuration.

As a proof of principle, we plot the integrated scattered intensity, integrated over the whole area of the AGIPD detector [14], against both normalization signals (Fig. 5). First, it is evident that either of the signals is valid for normalization as the integrated detector intensity I_{int} is linearly related to both with correlation coefficients of 0.99 and 0.98 for the diamond and photodiode detector, respectively. This holds for the observed range of incoming intensities that varied stochastically by about one order of magnitude. Normalization to the diamond signal leads to approximately a factor of 2 lower spread as compared to normalization to the signal from the photodiode. Hence, normalization by the former signal might be seen as superior. While this is evidently true for the situation shown here, this does not hold for every situation. Upon transmission through the diamond detector located upstream of the sample small-angle scattering is produced, especially at smaller q than was accessible here, using the AGIPD detector. In low-count-rate experiments, this can obscure the actual signal, making the measurements impossible.

3. Conclusion

We have presented a simple and reliable way to normalize scattering data taken at FEL sources by measuring signals from the beam transmitted through the sample using photodiodes. Fluctuations in the FEL intensity at the sample position including those produced by pointing instabilities or by using a monochromator upstream are monitored to a large extent. In an experiment at FLASH, using the signal from the transmitted beam leads to superior normalization of the data compared to using the FLASH GMD data. At European XFEL, normalization by means of a diamond intensity monitor upstream or the photodiode downstream of the sample led to comparable results. However, the upstream intensity monitor produces stray radiation around the direct beam that can be stronger than the actual measurement signal in SAXS experiments, such that monitoring intensity downstream of the sample may be preferable here as well. Note that all measurements have been conducted using single bunches per train at a

low repetition rate of 10 Hz, and an attenuated or monochromatized beam. In this configurations no indication of non-linearity was found. However, limitations when using megahertz repetition rates or high-intensity beams are expected due to saturation effects or signal build-up during a bunch train.

Acknowledgments

We acknowledge DESY (Hamburg, Germany), a member of the Helmholtz Association HGF, for the provision of experimental facilities. Parts of this research were carried out at FLASH beam line BL3. Equally, we acknowledge European XFEL in Schenefeld, Germany, for provision of X-ray free-electron laser beam time at the MID instrument. We would like to thank all involved staff for support.

We would like to acknowledge funding by the Deutsche Forschungsgemeinschaft (DFG, German Research Foundation) – SFB-925 – project 170620586.

References

- [1] Seddon E A, Clarke J A, Dunning D J, Masciovecchio C, Milne C J, Parmigiani F, Rugg D, Spence J C H, Thompson N R, Ueda K, Vinko S M, Wark J S and Wurth W 2017 *Rep. Prog. Phys.* **80** 115901
- [2] Nagler B, Zastra U, Faeustlin R R, Vinko S M, Whitcher T, Nelson A J, Sobierajski R, Krzywinski J, Chalupsky J, Abreu E, Bajt S, Bornath T, Burian T, Chapman H, Cihelka J, Doeppner T, Duesterer S, Dzelzainis T, Fajardo M, Foerster E, Fortmann C, Galtier E, Glenzer S H, Goede S, Gregori G, Hajkova V, Heimann P, Juha L, Jurek M, Khattak F Y, Khorsand A R, Klinger D, Kozlova M, Laarmann T, Lee H J, Lee R W, Meiwes-Broer K H, Mercere P, Murphy W J, Przystawik A, Redmer R, Reinholz H, Riley D, Roepke G, Rosmej F, Saksl K, Schott R, Thiele R, Tiggesbaeumker J, Toleikis S, Tschentscher T, Uschmann I, Vollmer H J and Wark J S 2009 *Nat. Physics* **5** 693–696
- [3] Müller L, Gutt C, Pfau B, Schaffert S, Geilhufe J, Büttner F, Mohanty J, Flewett S, Treusch R, Düsterer S, Redlin H, Al-Shemmary A, Hille M, Kobs A, Frömter R, Oepen H P, Ziaja B, Medvedev N, Son S K, Thiele R, Santra R, Vodungbo B, Lüning J, Eisebitt S and Grübel G 2013 *Phys. Rev. Lett.* **110** 234801
- [4] Cerantola V, Rosa A D, Konopkova Z, Torchio R, Brambrink E, Rack A, Zastra U and Pascarelli S 2021 *J. Phys.: Condens. Matter* **33** 274003
- [5] Tiedtke K, Azima A, von Barga N, Bittner L, Bonfigt S, Düsterer S, Faatz B, Fühling U, Gensch M, Gerth C, Guerassimova N, Juranic P, Kapitzki S, Keitel B, Kracht T, Kuhlmann M, Li W B, Martins M Núñez T, Plönjes E, Redlin H, Saldin E L, Schneidmiller E A, Schneider J R, Schreiber S, Stojanovic N, Tavella F, Toleikis S, Treusch R, Weigelt H, Wellhöfer M, Wabnitz H, Yurkov M V and Feldhaus J 2009 *New J. Phys.* **11** 023029
- [6] Macias I J B, Düsterer S, Ivanov R, Liu J, Brenner G, Rönsch-Schulenburg J, Czwalinna M K and Yurkov M V 2021 *Opt. Express* **29** 10491–10508
- [7] Madsen A, Hallmann J, Ansaldi G, Roth T, Lu W, Kim C, Boesenberg U, Zozulya A, Moeller J, Shayduk R, Scholz M, Bartmann A, Schmidt A, Lobato I, Sukharnikov K, Reiser M, Kazarian K and Petrov I 2021 *J. Synchrotron Radiat.* **28** 637–649
- [8] Stöhr J and Scherz A 2015 *Phys. Rev. Lett.* **115** 107402
- [9] Yoneda H, Inubushi Y, Yabashi M, Katayama T, Ishikawa T, Ohashi H, Yumoto H, Yamauchi K, Mimura H and Kitamura H 2014 *Nat. Commun.* **5** 5080
- [10] Beaupaire E, Merle J C, Daunois A and Bigot J Y 1996 *Phys. Rev. Lett.* **76** 4250–4253
- [11] Jeppson S and Kukreja R 2021 *APL Mater.* **9** 100702
- [12] Riepp M, Philippi-Kobs A, Müller L, Rysov R, Marotzke S, Walther M, Roseker W and Grübel G 2022 Temperature dependence of the energy equilibration time in laser-excited magnetic thin films — To be submitted
- [13] Roth T, Freund W, Boesenberg U, Carini G, Song S, Lefeuvre G, Goikhman A, Fischer M, Schreck M, Grünert J and Madsen A 2018 *J. Synchrotron Radiat.* **25** 177–188
- [14] Allahgholi A, Becker J, Delfs A, Dinapoli R, Goettlicher P, Greiffenberg D, Henrich B, Hirsemann H, Kuhn M, Klanner R, Klyuev A, Krueger H, Lange S, Laurus T, Marras A, Mezza D, Mozzanica A, Niemann M, Poehlsen J, Schwandt J, Sheviakov I, Shi X, Smoljanin S, Steffen L, Sztuk-Dambietz J, Trunk U, Xia Q, Zeribi M, Zhang J, Zimmer M, Schmitt B and Graafsma H 2019 *J. Synchrotron Radiat.* **26** 74–82